Program Digest, 2019 IEEE International Ultrasonics Symposium (IUS)
Glasgow, Scotland, October 6-9, 2019

Investigation of Energy Trapping of the Lateral Field Excited Thickness Shear Mode in AT-Cut Quartz Crystal Microbalances

Jequil S. R. Hartz, John F. Vetelino, *IEEE Life Fellow*
Frontier Institute for Research in Sensor Technology
University of Maine
Orono, Maine USA
jequil.hartz@maine.edu, john.vetelino@maine.edu

Nuri W. Emanetoglu, *IEEE Member*
Department of Electrical & Computer Engineering
University of Maine
Orono, Maine USA
nuri.emanetoglu@maine.edu

***Abstract*—Methods for improved energy trapping of the thickness shear mode (TSM) in quartz crystal microbalances (QCMs) under lateral field excitation (LFE) are presented. The dependencies of TSM resonant intensity and spurious mode presence on surface curvature and electrode geometry are analyzed for improved LFE QCM response. TSM resonance trend data are given for 6 MHz plano-convex uncoated wafers and electroded devices up to 6 diopters (D). The energy trapping concept is also extended to include electrical energy redistribution, which alters the active acoustic modes in LFE devices. Aspects of data on newly discovered metal-loaded LFE shear modes more intense than known LFE TSMs are presented. Variations of these metal-loaded device responses with surface curvature and metal layer thickness are reported. Butterworth-Van Dyke (BVD) equivalent circuit parameters are extracted for air- and metal-loaded response comparisons. The observed influences of acoustic and electrical energy trapping expand knowledge on the extent of LFE device capabilities and reveal implications for resonator applications.**

***Index Terms*—lateral field excitation, quartz crystal microbalance, energy trapping, bulk acoustic wave sensor**

I. Introduction

Thickness field excited (TFE) AT-cut quartz crystal microbalances (QCMs) are bulk acoustic wave (BAW) devices used in a wide range of sensing applications. AT-cut QCMs are used with oscillators tuned only to the pure temperature-compensated thickness shear mode (TSM), where the oscillation frequency shifts with mechanical loading (thickness/mass or viscosity). Commercial TFE QCM electrode placement also provides strong central confinement of electrical and acoustic energy, allowing excellent sensing system integration.

TFE QCMs, however, are unable to detect electrical changes (conductivity or permittivity) without a significant reduction in sensing surface electrode coverage. In contrast, lateral field excited (LFE) QCMs already exhibit superior electrical sensing capabilities [1] as greater electric field penetration into the target layer occurs. For TFE QCMs, the driving field is directed through the QCM thickness, whereas the field can be oriented in any direction in the lateral plane for LFE QCMs. The active BAW modes then depend on this field orientation, rather crystal cut. Certain modes may or may not be unique to only one of these excitations. For AT-cut quartz, the pure TSM can be isolated in both LFE and TFE QCMs.

Though more versatile, LFE QCMs are currently inferior to TFE QCMs due to high motional resistances, low coupling, and lesser energy trapping. Usual LFE electrodes [2] are incompatible with acoustic energy trapping without electrode modification [3] or QCM surface variation. Electrode geometries have been studied for better acoustic trapping [4] and mode excitation [5], but little data exist for surface variation of LFE QCMs. For LFE devices, different loadings have also introduced new energy trapping mechanisms based on electric field redistribution [6], expanding upon known energy trapping aspects [7]. However, only recently have metal layers been explored [8], with AT-cut quartz data currently unavailable.

The present work investigates the impacts of surface curvature and/or electrode geometry on spurious modes and both shear mode intensities of 6 MHz AT-cut quartz wafers for sensing applications. Thin ($< 1.5\ \mu$m) metal layer influence on mode generation and energy trapping is also studied. The Butterworth-Van Dyke (BVD) model [2] is used to compare electrical parameters. Suggestions for future sensing methodologies of AT-cut LFE QCMs are also discussed.

II. Theory

A. Lateral Field Excitation of AT-Cut Quartz

The BAW mode characteristics of the (YXl) 35.25° AT-cut of left-handed quartz were obtained with constants from [9]. The $x' - y' - z'$ system rotated relative to the crystallographic $x - y - z$ system defines the plate. The driving field is applied through the plate thickness along y' for TFE and in the $x'z'$ plane for LFE. The pure TSM displacement is along x' while the quasi modes deviate approximately 3.42° from the pure longitudinal y' and shear z' directions.

QCM modes have characteristic series and parallel resonant frequencies and overtones based on their immittances, which contain terms known as the electromechanical coupling coefficients, k^2. As shown by the k^2 values not identically zero [10] in Figure 1, TFE excites only the pure TSM, but all modes can be excited via LFE. Values in Figure 1 depend only on crystal

978-1-7281-4595-2/19/$31.00 ©2019 IEEE

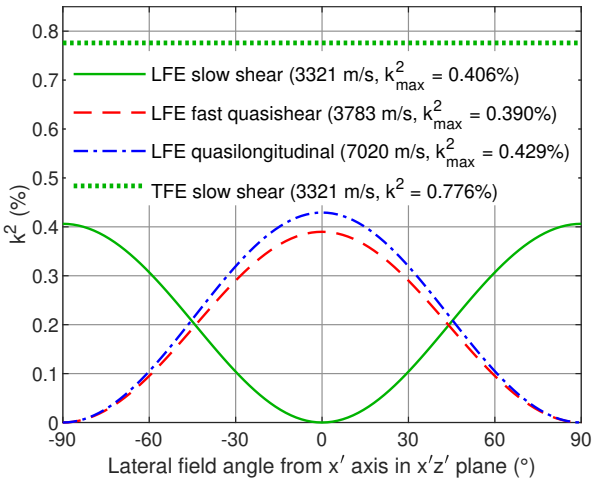

Figure 1. TFE and LFE mode electromechanical couplings for AT-cut quartz.

parameters, but the measured values may vary depending on the electrical interrogation of the response.

B. Acoustic and Electrical Energy Trapping

BAW TSMs depend only on plate thickness, but they are cut-offs of laterally-varying thickness-shear (TS) and (TT) modes, which couple to flexural (F), extensional (E), and face-shear (FS) plate modes dependent on the plate lateral dimensions [7]. Spurious modes near the TSMs include F, E, FS, and undesired TS and TT modes. TS and TT mode trapping can be adjusted by varying the cut-off frequencies along the plate though mass layers or variable crystal thickness, but the plate modes can only be eliminated for specific plate aspect ratios.

Acoustic energy of an air-loaded LFE device is mostly confined by the electrode gap, but the driving electric field can extend well beyond the surface, depending on crystal permittivity [11]. Electrical layers trap and redistribute this energy within the crystal, which alters mode generation as seen for water-loaded pseudo- and quasi-LFE [12] modes. Bound charges in dielectrics like water polarize near the gap to oppose the electrode charges, augmenting the thickness electric field component. Resonant energy then passes as mutual capacitive coupling between two TFE regions [13]. Direct energy transfer through the crystal (pure LFE) persists to a lesser extent. Mainly centralized redistribution has been observed with water, but metal layers can relocate charge away from the gap.

III. Device Fabrication and Measurement Setup

13.97 mm (0.55″) 6 MHz AT-cut plano-convex blank quartz wafers with flats indicating the z'-axis were obtained from Fil-Tech, Inc. (Boston, MA). Surface curvatures varied from 0 (plano-plano) to 6 diopters (D) in unit steps. Half-moon [2] electrodes were considered with 9, 11 and 13 mm diameters in combination with 0.5, 1.5, and 2.5 mm gaps. Electrodes consisted of 200 Å Cr and 2000 Å Au. Electroded devices have currently been fabricated only for slow TSM excitation.

All measurements were taken within a controlled cleanroom environment to eliminate potential extraneous factors. Printed

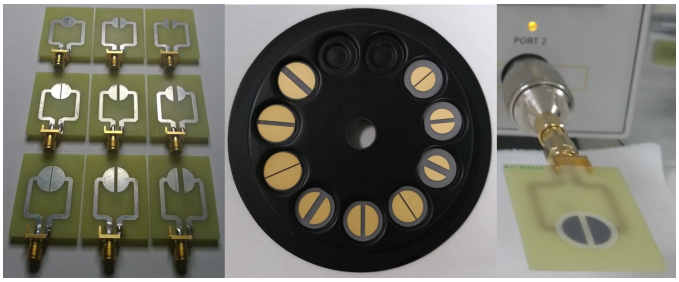

Figure 2. (From left to right) PCBs, electroded device configurations, and LFE QCM single port measurement.

circuit board (PCB) electrodes, electroded devices, and a single port measurement on an E5071C network analyzer with PCB excitation are shown in Figure 2. No extra physical loading was applied during measurement, and all samples were centered on the PCB electrodes to ensure maximal central excitation. For uncoated wafers, the active modes varied by rotating the crystal on the PCB. Admittance data were obtained for uncoated wafers and all electrode combinations for each diopter.

The magnitude and phase shifts of data were used to determine response intensity. The magnitude shift indicated resemblance of the response to an ideal lossless resonator, while phase shift necessary for standard oscillator circuit integration is 180°. The BVD model was used to extract equivalent circuit parameters. Additionally, 6 MHz TFE QCMs were measured with a thin film deposition system sensing arm for reference.

IV. Results and Discussion

A. Air-loaded LFE response

For uncoated wafers rated at 6.02 - 6.04 MHz, the quasi mode fundamental frequencies are between 6.8575 - 6.8803 MHz (fast TSM) and 12.7252 - 12.7675 MHz. Modes were active in the predicted frequency ranges when the PCB was rotated. Quasilongitudinal mode response was weak with several adjacent spurious modes, making the mode unsuitable for sensing. The 0D TSM responses were similar, but 1D curvature focused the resonances for both TSMs. The TSM intensities were very

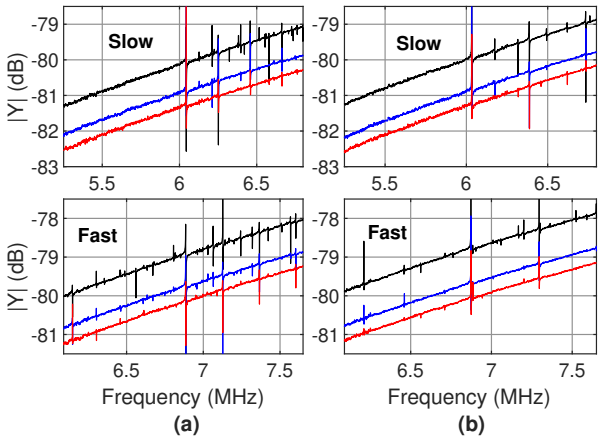

Figure 3. Diopter and gap width impact on spurious modes for both TSMs in (a) 2D and (b) 6D uncoated wafers. Increasing gap width from top to bottom.

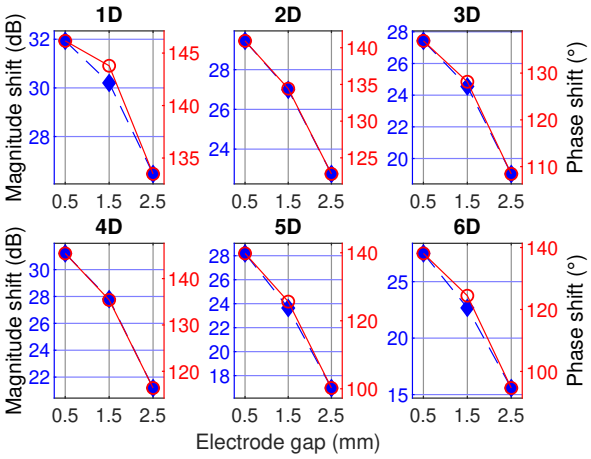

Figure 4. Magnitude (dashed line with diamond) and phase shift (solid line with circle) diopter trends for electrode gap with 9 mm diameter.

similar; however, the spurious modes near the TSMs differed. Excluding 0D, the pure TSM had no spurious modes both below resonance and at least 80 kHz above. For the fast TSM, spurious modes were present below and above the mode, with a robust spurious mode appearing near the main mode for 5D.

For both TSMs, spurious modes vanished for larger PCB electrode gaps, as shown in Figure 3. Increasing diopter also reduced spurious modes, as shown from the comparison of Figures 3(a) and 3(b). Both TSM intensities largely increased with decreasing electrode gap (Figure 4) as gap field intensity rose. Weakest responses consistently occurred for 5D and 6D.

Only 9 mm diameter PCB data are included in Figure 4 as PCB electrode diameter did not impact previous trends. The same holds for attached electrodes as the curvature had greater impact than the electrode lateral extent. However, electroded devices did not produce the trends in Figure 4 due to conflicting acoustic trapping of electroded regions and curvature. Though electroded devices were only 3% weaker in intensity on average, the standard deviation in electroded/uncoated response ratio was roughly 18%. The 9 mm diameter, 0.5 mm gap electrode pattern was chosen for successive deposition and PCB excitation for strongest responses and least electrode presence.

From lesser spurious activity, only pure TSM BVD parameters were reliably extracted. With peak coefficient of variation of 0.119, the average motional resistance (R_m), static capacitance (C_0), motional capacitance (C_m), and k^2 were 1.84 kΩ, 2.65 pF, 0.0658 fF, and 0.00306%, respectively. The TFE QCM had R_m and k^2 as 15.8 Ω and 0.0210%, respectively. The best air-loaded magnitude and phase shifts were 32.0 dB and 146°, compared to the TFE QCM values of 55.8 dB and 171°. Accordingly, sensor feasibility of air-loaded LFE QCMs is limited without more sophisticated resonance tracking [14].

B. Metal-loaded LFE response

Resonances stronger than previously observed LFE modes in Figure 5 occurred with a 20 nm thick, 6.35 mm (0.25˝) diameter circle Cr centrally applied to electroded device sensing surfaces. These resonances were not at either TSM frequency

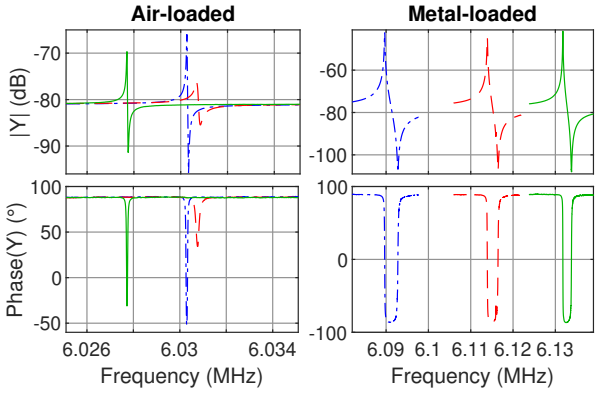

Figure 5. Air- and metal-loaded responses for 2D (dot-dashed curves), 3D (dashed curves), and 4D (solid curves) electroded devices.

but within 100 kHz of the slow TSM. From Figure 5, the effective crystal thickness impacted resonance like a thickness mode. The responses also consistently showed larger response shifts (around 62.8 dB and 175°) than their usual LFE and TFE counterparts. From Figure 6, a similar mode arose less than 20 kHz higher in 2D wafers when rotated on a PCB. The modes were designated as 0° and 90° LFE modes (Figure 6(a)). For the 0° mode, the crystal flat is aligned with the field direction, and the 90° mode appears when rotated 90°. When excited at 45° (Figure 6(b)), energy is shared between these modes equally. For only 20 nm Cr, the usual LFE modes were also found hardly active at their respective frequencies. HFSS simulation indicates electrical paths through the electrode gap and the metal layer boundary, inducing both thickness and radial lateral field components. From closeness to the slow TSM and no spurious modes below resonance, these modes could be the TFE pure TSM augmented by the lateral field.

Cr thickness for 0D and 1D samples was gradually increased to observe the metal layer effect at the limit of curvature necessary for acoustic trapping. Usual mass frequency shifts happened, but variation in Cr centering generated spurious modes for both the 0D modes and the 1D 90° mode. A

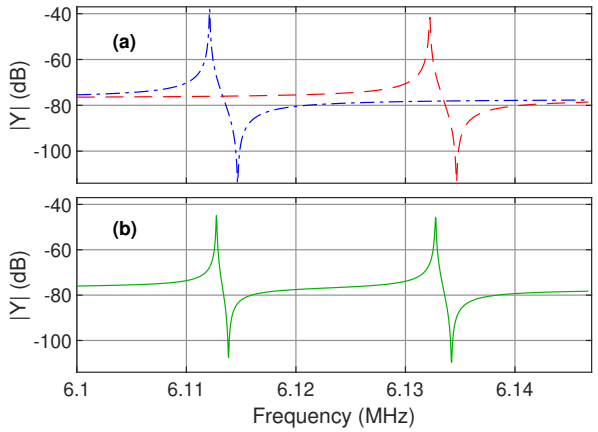

Figure 6. Energy trading of metal-loaded modes at (a) 0° (dot-dashed curve) and 90° (dashed curve) and (b) energy sharing when at 45° (solid curve).

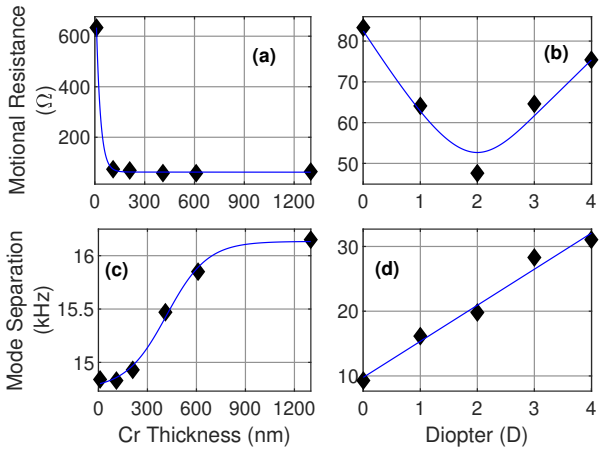

Figure 7. Approximate trends of motional resistance and mode separation vs. (a) & (c) Cr thickness and (b) & (d) diopter for 1300 nm Cr load.

0D resonance did improve with increasing Cr thickness, but substantial mode isolation only happened for 1300 nm thickness. Thus, it is possible to focus the 0D response with mixed mass and electrical loading. The minor spurious presence near the 1D 90° mode could be attributed to lateral mode coupling differences previously seen for the usual LFE TSMs. Increasing diopter removes these minor spurious modes, confirmed from observations of 2D, 3D, and 4D wafers loaded with 1300 nm Cr. With spurious modes present for lower Cr loads, Cr thickness trends for just the 0° mode were examined.

R_m varied significantly with Cr thickness. As Cr thickness increased, R_m approached 50 Ω, as shown in Figure 7(a). Minimum R_m of 47.6 Ω occurred for 2D (Figure 7(b)). C_s and C_m were 0.360 pF and 0.378 fF, respectively, expressing greater electric field trapping and acoustic wave activity. k^2 value of 0.130% was closer to usual AT-cut quartz values. With great improvement from thin metal layers, there is obvious utility for LFE QCMs in contact-less metal layer sensing [8]. The observed trends could be incorporated into sensing with frequency shifts used for the QCM. With nearly 180° of phase shift, conventional oscillators can also be used.

Increasing Cr thickness was also discovered to separate the 0° and 90° modes sigmoidally (Figure 7(c)) due to increasing layer conductance. The mode separation also increased linearly with diopter for wafers loaded (Figure 7(d)), as expected from reduced average crystal thickness. With high coupling in tandem with adjustable mode presence and separation, fewer resonators could be used for RF filter applications.

V. Conclusions

Energy trapping and mode generation aspects of air- and metal-loaded LFE AT-cut QCMs have been reported. Both TSMs were of similar intensity with distinct spurious mode activity. Surface curvature and electrode gap showed the greatest acoustic trapping impact, with attached electrodes presenting adverse acoustic trapping behavior for the diameters tested. Trade-off between spurious mode presence and excitation intensity with the electrode gap occurred. Increased surface curvature also reduced spurious mode presence; however, diopters larger than 4D produced weaker responses and greater device fragility. BVD parameters hardly varied for air-loaded uncoated wafers, with poor coupling and high motional resistance.

Thin metal layer presence produced new LFE modes with tunable motional resistance and mode separation dependent on metal thickness and diopter, with preserved high coupling. Metal-loaded responses also surpassed TFE QCM responses, improving LFE QCM sensor system feasibility near metal layers. From the trends for Cr thickness, there are new possible methodologies for tracking the sensor response of a QCM. With metal-loaded modes revealed for AT-cut quartz, there also exist opportunities for discovery or design of similar modes in higher coupling piezoelectric materials for resonator applications. Furthermore, different LFE resonant property changes from sensing surface metal geometry may be investigated.

Acknowledgment

This work was funded by National Science Foundation PFI:AIR - TT: Lateral Field Excited Acoustic Wave Sensor for Monitoring Thin Film Properties in Solid State Devices. Jequil Hartz acknowledges support by Dr. George Bernhardt, Michael Call, Bailee Bartash, Jackson Hall, and Armando Ayes.

References

[1] J. F. Vetelino, "A Lateral Field Excited Acoustic Wave Sensor Platform," in *Proc. IEEE Int. Ultrason. Symp.*, 2010, pp. 924–934.
[2] J. Vetelino and A. Reghu, *Introduction to Sensors*, 2011.
[3] W. Wang, C. Zhang, Z. Zhang, T. Ma, and G. Feng, "Energy-trapping mode in lateral-field-excited acoustic wave devices," *Appl. Phys. Lett.*, vol. 94, no. 19, 2009.
[4] T. Ma, C. Zhang, W. Wang, Z. Zhang, and G. Feng, "Optimal Electrode Shape and Size of Lateral-Field-Excited Piezoelectric Crystal Resonators," *IEEE Trans. Ultrason. Ferroelectr. Freq. Control*, vol. 58, no. 1, pp. 263–266, 2011.
[5] W. Wang, Z. Zhang, C. Zhang, Y. Liu, G. Feng, and G. Jing, "Novel electrode configurations of lateral field excited acoustic wave devices on (yxl)-58° LiNbO3," in *Proc. IEEE Int. Ultrason. Symp.*, 2008, pp. 276–279.
[6] U. Hempel, R. Lucklum, P. R. Hauptmann, E. P. Eernisse, D. Puccio, and R. F. Diaz, "Quartz crystal resonator sensors under lateral field excitation - a theoretical and experimental analysis," *Meas. Sci. Technol.*, vol. 19, no. 5, 2008.
[7] J. Yang, *Vibration of Piezoelectric Crystal Plates*, 2013.
[8] B. D. Zaitsev, A. M. Shikhabudinov, A. A. Teplykh, and I. A. Borodina, "The influence of the metal film, placed close to the free side of the piezoelectric lateral electric field excited resonator, on its characteristics," *Ultrasonics*, vol. 84, pp. 107–111, 2018.
[9] B. J. James, "New Measurement of the Basic Elastic and Dielectric Constants of Quartz," in *Proc. 42nd Annu. IEEE Int. Freq. Control Symp.*, 1988, pp. 146–154.
[10] A. Ballato, "Extended Christoffel-Bechmann Elastic Wave Formalism for Piezoelectric, Dielectric Media," in *Proc. IEEE/EIA Int. Freq. Control Symp. Exhib.*, 2000, pp. 340–344.
[11] J. Fochtmann, C. Peters, R. F. Diaz, R. Lucklum, J. McGann, J. Vetelino, and A. Arnau, "Simulation and measurement of low permittivity media with LiNbO3 and LiTaO3 LFE resonators," in *Proc. IEEE Int. Freq. Control Symp.*, 2010, pp. 365–370.
[12] W. Wang, Z. Zhang, C. Zhang, Y. Liu, G. Feng, and G. Jing, "Three operation modes of acoustic wave devices with a lateral field excitation structure," in *Proc. IEEE Int. Ultrason. Symp.*, 2008, pp. 443–446.
[13] ——, "Pseudo-LFE study in AT-cut quartz for sensing applications," in *Proc. IEEE Sensors*, 2008, pp. 1548–1551.
[14] T. J. Leighton, "Development of an Electrical Interface for A Lateral Field Excited Sensor System," M. S. Thesis, University of Maine, 2019.